

## A Factorizable Formulation of Tight Binding

EARL E. LAFON

*Department of Physics, Oklahoma State University, Stillwater, Oklahoma 74078*

Received March 18, 1987; revised September 23, 1988

A compact mathematical formulation for *ab initio* tight binding calculations of the electronic band structure of crystalline materials is presented. Within this formulation it is shown that, for a large number of crystals, the multicenter integrals, *per se*, do not need to be calculated. This results in a considerable savings in computational effort and greatly reduces the amount of information which must be stored. These advantages are of particular importance in supercell calculations such as those encountered in investigating the electronic structure of surfaces and interfaces. © 1989 Academic Press, Inc.

### I. INTRODUCTION

The first principles calculation of the electronic structure of crystalline materials by the method of tight binding or linear combination of atomic orbitals (LCAO) first presented by Bloch in 1928 [1] has enjoyed considerable success over the last twenty years [2]. During this time it has been clearly demonstrated that this method is capable of accurately predicting the band structure and associated bulk properties of not only the so-called “tightly-bound” systems but also of the “free-electron” materials as well [3–5].

As we move into the study of surface states [6] and other phenomena requiring large numbers of atoms within the unit cell, one of the most outstanding advantages of tight binding is its ability to accurately predict the electronic structure with an extremely small number of basis functions per atom. Since the number of basis functions is proportionately small, this means that systems which contain large numbers of atoms within the unit cell can be investigated while still employing only moderately large secular equations. There are two major difficulties still encountered in performing a tight binding calculation with large numbers of atoms within the unit cell.

The first problem is centered about the sometimes excessive amount of machine time needed to calculate (and the disk space to store) the enormous number of multicenter integrals required for a truly accurate treatment of the electronic structure of these materials. This is especially true in surface calculations where a long slender rectangular (orthorhombic) unit cell is employed, and yet a multitude of *k*-points within the 2-dimensional Brillouin zone must be investigated. In the following sections, a factorized tight binding formulation (FTB) is presented. The FTB

formalism employs a novel computational strategy which effectively reduces an  $N^3$  problem into a  $3N$  problem. In materials involving rectangular unit cells (which is frequently the case in surface calculations), the FTB formalism does not even require the evaluation of the multicenter integrals *per se*. This drastically reduces the quantity of information which must be calculated and permanently stored. The program development described in the following sections takes full advantage of the FTB formalism. Although these programs are general in nature and entirely independent of crystalline symmetry, it is in the area of thin films, surface states, and interfaces that the FTB formalism excels.

The second difficulty is principally centered about the problems involved in achieving true self-consistency when the number of atoms within the unit cell is large. For problems of the bulk, nonself-consistent calculations frequently work quite well, but the same cannot be said for problems involving thin films where one would expect considerable rearrangement of the bulk charge distribution as one approaches the surface. The FTB formalism appears to be ideally suited for extension to self-consistency. Additionally, the same general philosophy of factorization can also be applied to calculations of the crystalline charge density.

## II. BASIC NOMENCLATURE AND TIGHT BINDING FORMULATION

In this paper Hartree atomic units will be used throughout unless stated otherwise. The three primitive lattice vectors will be denoted by  $\mathbf{a}_1$ ,  $\mathbf{a}_2$ , and  $\mathbf{a}_3$ . A general lattice point is then given by

$$\mathbf{R}_v = v_1 \mathbf{a}_1 + v_2 \mathbf{a}_2 + v_3 \mathbf{a}_3, \quad (2.1)$$

where

$$v = (v_1, v_2, v_3), \quad v_i = \text{integer.}$$

The central unit cell with edges  $\mathbf{a}_1$ ,  $\mathbf{a}_2$ ,  $\mathbf{a}_3$  and volume  $\Omega$  may contain many atoms each with atomic number  $Z_j$  and position  $\mathbf{t}_j$ . The reciprocal lattice vectors,  $\mathbf{K}_\mu$ , are written as

$$\mathbf{K}_\mu = \mu_1 \mathbf{b}_1 + \mu_2 \mathbf{b}_2 + \mu_3 \mathbf{b}_3, \quad (2.2)$$

where

$$\mu = (\mu_1, \mu_2, \mu_3), \quad \mu_i = \text{integer,}$$

and where

$$\mathbf{b}_i = 2\pi \mathbf{a}_j \times \mathbf{a}_k / \Omega, \quad i, j, k = \text{cyclic permutation of } 1, 2, 3. \quad (2.3)$$

The single particle Hamiltonian is written as

$$\mathcal{H} = -\frac{1}{2}\nabla^2 + V(\mathbf{r}), \quad (2.4)$$

where the effective crystalline potential,  $V(\mathbf{r})$ , exhibits the periodicity of the lattice:

$$V(\mathbf{r} + \mathbf{R}_v) = V(\mathbf{r}). \quad (2.5)$$

In addition, the crystalline potential is assumed here, without loss of generality, to be written in the form

$$V(\mathbf{r}) = V^c(\mathbf{r}) + V^g(\mathbf{r}) + V^k(\mathbf{r}), \quad (2.6)$$

where

$$V^c(\mathbf{r}) = \sum_v \sum_j U_j^c[\mathbf{r} - (\mathbf{R}_v + \mathbf{t}_j)], \quad (2.7)$$

$$V^g(\mathbf{r}) = \sum_v \sum_j U_j^g[\mathbf{r} - (\mathbf{R}_v + \mathbf{t}_j)], \quad (2.8)$$

$$V^k(\mathbf{r}) = \sum_\mu U_\mu^k(\mathbf{C}) e^{i\mathbf{K}_\mu \cdot \mathbf{r}\mathbf{C}}, \quad (2.9)$$

and where

$$U_j^c(\mathbf{r}) = -Z_j e^{-\delta r^2/r}, \quad (2.10)$$

$$U_j^g(\mathbf{r}) = \sum_\gamma \sum_{nlm} \sigma_j^{nlm}(\gamma) \chi_{nlm}(\gamma, \mathbf{r}), \quad (2.11)$$

$$\chi_{nlm}(\gamma, \mathbf{r}) = x^n y^l z^m e^{-\gamma r^2}. \quad (2.12)$$

Since the decomposition of Eq. (2.6) is not unique,  $V^g(\mathbf{r})$  is chosen in such a manner as to make the Fourier components,  $U_\mu^k$ , as small and as rapidly convergent as is reasonably possible. As a result,  $V^k(\mathbf{r})$  can usually be ignored in nonself-consistent calculations of the bulk.

The variational wave function is written as an expansion of Bloch functions formed from Gaussian orbitals

$$\psi(\mathbf{k}, \mathbf{r}) = \sum_j \sum_i \sum_{nlm} C_{j i nlm}^{nlm}(\alpha_i, \mathbf{k}) b_{nlm}^j(\alpha_i, \mathbf{k}, \mathbf{r}), \quad (2.13)$$

where

$$b_{nlm}^j(\alpha_i, \mathbf{k}, \mathbf{r}) = N^{-1/2} \sum_v e^{i\mathbf{k} \cdot \mathbf{R}_v} \chi_{nlm}[\alpha_i, \mathbf{r} - (\mathbf{R}_v + \mathbf{t}_j)], \quad (2.14)$$

and where  $N$  stands, symbolically, for the number of unit cells in the crystal. The orbital exponents,  $\alpha_i$ , are usually obtained from atomic or atomic-like solutions

based on the isolated individual atoms. Usually, certain constraints are placed on the variational parameters. These constraints are of the form

$$\sum_j \sum_i \sum_{nlm} d_{nlm}^j(\alpha_i, \mathbf{k}) C_j^{nlm}(\alpha_i, \mathbf{k}) = 0, \quad (2.15)$$

and usually arise from orbital contraction and core orthogonalization [2]. For simplicity, in this development such constraints will be ignored and the full variational freedom of Eq. (2.13) will be preserved.

Application of the variational principle leads to the familiar secular equation of the form

$$|H - ES| = 0, \quad (2.16)$$

where the  $i$ th root,  $E_i$ , is an upper bound to the  $i$ th band [7] for the Hamiltonian given by Eq. (2.4). The matrix elements contained in Eq. (2.16) are given by

$$\begin{aligned} O_{n_1 l_1 m_1, n_2 l_2 m_2}(\alpha_1, \alpha_2, \mathbf{k}) &= \int b_{n_1 l_1 m_1}^{j_1}(\alpha_1, \mathbf{k}, \mathbf{r}) \mathcal{O} b_{n_2 l_2 m_2}^{j_2}(\alpha_2, \mathbf{k}, \mathbf{r}) d\tau \\ &= \sum_{\mathbf{v}} e^{i\mathbf{k} \cdot \mathbf{R}_{\mathbf{v}}} \int \chi_{n_1 l_1 m_1}(\alpha_1, \mathbf{r} - \mathbf{t}_{j_1}) \mathcal{O} \chi_{n_2 l_2 m_2}[\alpha_2, \mathbf{r} - (\mathbf{R}_{\mathbf{v}} + \mathbf{t}_{j_2})] d\tau \\ &= \sum_{\mathbf{v}} e^{i\mathbf{k} \cdot \mathbf{R}_{\mathbf{v}}} O_{n_1 l_1 m_1, n_2 l_2 m_2}(\alpha_1, \alpha_2, \mathbf{t}_{j_1}, \mathbf{R}_{\mathbf{v}} + \mathbf{t}_{j_2}), \end{aligned} \quad (2.17)$$

where

$$O_{n_1 l_1 m_1, n_2 l_2 m_2}(\alpha_1, \alpha_2, \mathbf{A}, \mathbf{B}) = \int \chi_{n_1 l_1 m_1}(\alpha_1, \mathbf{r}_A) \mathcal{O} \chi_{n_2 l_2 m_2}(\alpha_2, \mathbf{r}_B) d\tau, \quad (2.18)$$

$$\mathbf{r}_A = \mathbf{r} - \mathbf{A},$$

$$\mathbf{r}_B = \mathbf{r} - \mathbf{B}.$$

The decomposition in Eq. (2.17) is valid for any operator  $\mathcal{O}$  which is invariant under all symmetry translations,  $\mathbf{R}_{\mathbf{v}}$ , of the lattice. In particular, when  $\mathcal{O}$  is the operator  $\mathcal{H}$  of Eq. (2.4), then Eq. (2.17) yields the Hamiltonian matrix elements  $H$ , of Eq. (2.16), and when  $\mathcal{O}$  is the identity operator, then Eq. (2.17) gives the overlap matrix elements  $S$ .

### III. THE OVERLAP AND KINETIC ENERGY MATRIX ELEMENTS

The overlap and kinetic energy matrix elements are ultimately expressible by means of Eq. (2.17) as a lattice sum of two-center integrals of the form

$$S_{n_1 l_1 m_1, n_2 l_2 m_2}(\alpha_1, \alpha_2, \mathbf{A}, \mathbf{B}) = \int \chi_{n_1 l_1 m_1}(\alpha_1, \mathbf{r}_A) \chi_{n_2 l_2 m_2}(\alpha_2, \mathbf{r}_B) d\tau, \quad (3.1)$$

$$T_{n_1 l_1 m_1, n_2 l_2 m_2}(\alpha_1, \alpha_2, \mathbf{A}, \mathbf{B}) = \int \chi_{n_1 l_1 m_1}(\alpha_1, \mathbf{r}_A) \left(-\frac{1}{2}\nabla^2\right) \chi_{n_2 l_2 m_2}(\alpha_2, \mathbf{r}_B) d\tau, \quad (3.2)$$

where the notation of Eq. (2.18) is employed. These two-center integrals are easily evaluated and can be written as

$$S_{n_1 l_1 m_1, n_2 l_2 m_2}(\alpha_1, \alpha_2, \mathbf{A}, \mathbf{B}) = S_{n_1, n_2}(\alpha_1, \alpha_2, A_x, B_x) S_{l_1, l_2}(\alpha_1, \alpha_2, A_y, B_y) S_{m_1, m_2}(\alpha_1, \alpha_2, A_z, B_z), \quad (3.3)$$

$$T_{n_1 l_1 m_1, n_2 l_2 m_2}(\alpha_1, \alpha_2, \mathbf{A}, \mathbf{B}) = -\frac{1}{2} [ T_{n_1, n_2}(\alpha_1, \alpha_2, A_x, B_x) S_{l_1, l_2}(\alpha_1, \alpha_2, A_y, B_y) S_{m_1, m_2}(\alpha_1, \alpha_2, A_z, B_z) + S_{n_1, n_2}(\alpha_1, \alpha_2, A_x, B_x) T_{l_1, l_2}(\alpha_1, \alpha_2, A_y, B_y) S_{m_1, m_2}(\alpha_1, \alpha_2, A_z, B_z) + S_{n_1, n_2}(\alpha_1, \alpha_2, A_x, B_x) S_{l_1, l_2}(\alpha_1, \alpha_2, A_y, B_y) T_{m_1, m_2}(\alpha_1, \alpha_2, A_z, B_z) ], \quad (3.4)$$

where

$$S_{n_1, n_2}(\alpha_1, \alpha_2, A_x, B_x) = \exp(-H\overline{AB}_x^2) \sum_{r_1} \binom{n_1}{r_1} \overline{AD}_x^{n_1 - r_1} \sum_{r_2} \binom{n_2}{r_2} \overline{BD}_x^{n_2 - r_2} E_{r_1 + r_2}(\beta), \quad (3.5)$$

$$T_{n_1, n_2}(\alpha_1, \alpha_2, A_x, B_x) = n_2(n_2 - 1) S_{n_1, n_2 - 2}(\alpha_1, \alpha_2, A_x, B_x) - 2\alpha_2(2n_2 + 1) S_{n_1, n_2}(\alpha_1, \alpha_2, A_x, B_x) + 4\alpha_2^2 S_{n_1, n_2 + 2}(\alpha_1, \alpha_2, A_x, B_x), \quad (3.6)$$

where

$$\beta = \alpha_1 + \alpha_2, \quad H = \alpha_1 \alpha_2 / \beta, \quad \mathbf{D} = (\alpha_1 \mathbf{A} + \alpha_2 \mathbf{B}) / \beta, \quad \overline{AB}_x = B_x - A_x, \quad (3.7)$$

and where

$$E_n(\beta) = N_n \beta^{-(n+1)/2}, \quad N_n = \pi^{1/2} \begin{cases} 0 & \text{if } n = \text{odd} \\ \frac{(n-1)!!}{2^{n/2}} & \text{if } n = \text{even.} \\ 1 & \text{if } n = 0 \end{cases} \quad (3.8)$$

Usually the overlap and kinetic energy integrals are presented in such a manner that this factorization into  $x$ ,  $y$ , and  $z$  components is obscured [8, 9]. This factorization can be of great value. The lattice sum in Eq. (2.17) can be visualized as extending over all lattice site  $B$ -points within a sphere of radius  $R$  centered about point  $A$ . When  $\alpha_1$  and  $\alpha_2$  are small, the associated radius  $R$  is large and may include thousands of  $B$ -points for which the multicenter integrals must be evaluated. The number of  $B$ -points contained within a sphere of radius  $R$  is proportional to  $R^3$  but the number of unique values of  $B_x$ ,  $B_y$ , and  $B_z$  is, usually, proportional to  $R$ . Thus the matrices,  $S_{i,j}$ , can be precomputed for all unique values of  $B_x$ ,  $B_y$ ,  $B_z$  and the evaluation of the individual multicenter integrals reduces to just a few multiplications and additions of these precomputed quantities. For example, in the case of silicon an  $R$ -value of 27 results in more than 1000  $B$ -points. Within this sphere there are only 16 unique values of  $B_x$ ,  $B_y$ , and  $B_z$ . Consequently, only 16  $S$ -matrices must be precomputed and the more than 2000 integrals of overlap and kinetic energy can be rapidly evaluated from these precomputed quantities.

The above development shows that the overlap and kinetic energy integrals can be evaluated with great rapidity. The computational burden of tight binding, however, rests squarely on the integrals of potential energy—the overlap and kinetic energy integrals have never been a major problem. However, as will be shown in the next section, this same factorization exists in the multicenter integrals of potential energy where it can be used to double advantage.

#### IV. THE POTENTIAL ENERGY MATRIX ELEMENTS

##### A. The Matrix Elements of $V^g$

The expression for  $V^g$  given in Eq. (2.8) can be rewritten as

$$V^g(\mathbf{r}) = \sum_j \sum_\gamma \sum_{nlm} \sigma_j^{nlm}(\gamma) \mathbf{X}_{nlm}(\gamma, \mathbf{r} - \mathbf{t}_j), \quad (4.1)$$

where

$$\mathbf{X}_{nlm}(\gamma, \mathbf{r}) = \sum_v \chi_{nlm}(\gamma, \mathbf{r} - \mathbf{R}_v). \quad (4.2)$$

Using this notation, the multicenter integrals needed to evaluate the matrix element of  $V^g$  decomposes into a sum of the form

$$\begin{aligned} & V_{n_1 l_1 m_1, n_2 l_2 m_2}^g(\alpha_1, \alpha_2, \mathbf{A}, \mathbf{B}) \\ &= \sum_{j_3} \sum_\gamma \sum_{n_3 l_3 m_3} \sigma_{j_3}^{n_3 l_3 m_3}(\gamma) \mathbf{X}_{n_1 l_1 m_1, n_2 l_2 m_2}^{n_3 l_3 m_3}(\alpha_1, \alpha_2, \gamma, \mathbf{A}, \mathbf{B}, \mathbf{t}_{j_3}), \end{aligned} \quad (4.3)$$

where the notation of Eq. (2.18) has been employed and where

$$\begin{aligned} & \mathbf{X}_{n_1 l_1 m_1, n_2 l_2 m_2}^{n_3 l_3 m_3}(\alpha_1, \alpha_2, \gamma, \mathbf{A}, \mathbf{B}, \mathbf{C}) \\ &= \int \chi_{n_1 l_1 m_1}(\alpha_1, \mathbf{r}_A) \mathbf{X}_{n_3 l_3 m_3}(\gamma, \mathbf{r}_C) \chi_{n_2 l_2 m_2}(\alpha_2, \mathbf{r}_B) d\tau \\ &= \sum_{v'} \int \chi_{n_1 l_1 m_1}(\alpha_1, \mathbf{r}_A) \chi_{n_3 l_3 m_3}(\gamma, \mathbf{r}_C - \mathbf{R}_{v'}) \chi_{n_2 l_2 m_2}(\alpha_2, \mathbf{r}_B) d\tau. \end{aligned} \quad (4.4)$$

The individual three-center integrals can be easily evaluated to yield

$$\begin{aligned} & \int \chi_{n_1 l_1 m_1}(\alpha_1, \mathbf{r}_A) \chi_{n_3 l_3 m_3}(\gamma, \mathbf{r}_C) \chi_{n_2 l_2 m_2}(\alpha_2, \mathbf{r}_B) d\tau \\ &= U_{n_1 n_2}^{n_3}(\alpha_1, \alpha_2, \gamma, A_x, B_x, C_x) U_{l_1 l_2}^{l_3}(\alpha_1, \alpha_2, \gamma, A_y, B_y, C_y) \\ & \quad \times U_{m_1 m_2}^{m_3}(\alpha_1, \alpha_2, \gamma, A_z, B_z, C_z), \end{aligned} \quad (4.5)$$

where

$$\begin{aligned} & U_{n_1 n_2}^{n_3}(\alpha_1, \alpha_2, \gamma, A_x, B_x, C_x) \\ &= \exp(-H\overline{AB}_x^2) \exp(-G\overline{CD}_x^2) \\ & \quad \times \sum_{r_1} \binom{n_1}{r_1} \overline{AP}_x^{n_1-r_1} \sum_{r_2} \binom{n_2}{r_2} \overline{BP}_x^{n_2-r_2} \sum_{r_3} \binom{n_3}{r_3} \overline{CP}_x^{n_3-r_3} E_{r_1+r_2+r_3}(\lambda). \end{aligned} \quad (4.6)$$

and where

$$\lambda = \beta + \gamma, \quad \mathbf{P} = (\beta \mathbf{D} + \gamma \mathbf{C})/\lambda, \quad G = \beta\gamma/\lambda. \quad (4.7)$$

The sum over  $v'$  in Eq. (4.4) can be visualized as a sum over all  $C$ -points which lie within a sphere of radius  $R'$  centered about point  $D$ . The radius  $R'$  is primarily a function of the parameters  $H$  and  $G$ . If  $\alpha_1, \alpha_2$ , and  $\gamma$  are small, the number of  $C$ -points in the lattice sum over  $v'$  can be extremely large but, as was discussed in Section III, the number of unique values of  $C_x, C_y$ , and  $C_z$  is usually quite small. The  $U$ -matrices can be precomputed for these unique values and the evaluation of each three-center integral is then reduced to a pair of multiplications of these precomputed values.

Since the  $\sigma$ 's of Eq. (4.1) can be expected to change in each successive iteration toward self-consistency, it is best to evaluate and store away the individual  $\mathbf{X}$ -integrals for these need to be evaluated only once. The multicenter integrals of  $V^g$  in any given iteration can then be obtained from these precomputed  $\mathbf{X}$ -integrals using Eq. (4.3). This requires permanent storage of an extremely large number of integrals. This storage problem is significantly reduced if the unit cell has rectangular symmetry. In such a case, the multicenter integrals do not need to be evaluated and storage requirements are greatly reduced. This simplification will be discussed in detail in Section V.

### B. The Matrix Elements of $V^k$

The integrals involving  $V^k$  can be expressed as a reciprocal lattice sum over  $\mathbf{K}_\mu$  of multicenter integrals of the form

$$V_{n_1 l_1 m_1, n_2 l_2 m_2}^k(\alpha_1, \alpha_2, \mathbf{A}, \mathbf{B}, \mathbf{C}, \mathbf{K}_\mu) = \int \chi_{n_1 l_1 m_1}(\alpha_1, \mathbf{r}_A) \exp(i\mathbf{K}_\mu \cdot \mathbf{r}_C) \chi_{n_2 l_2 m_2}(\alpha_2, \mathbf{r}_B) d\tau, \quad (4.8)$$

where

$$\mathbf{r}_C = \mathbf{r} - \mathbf{C}$$

and where the point  $\mathbf{C}$  is some point in the lattice about which the Fourier series is expanded. Evaluation of this integral yields

$$V_{n_1 l_1 m_1, n_2 l_2 m_2}^k(\alpha_1, \alpha_2, \mathbf{A}, \mathbf{B}, \mathbf{C}, \mathbf{K}_\mu) = K_{n_1, n_2}(\alpha_1, \alpha_2, A_x, B_x, C_x, K_{\mu x}) \times K_{l_1, l_2}(\alpha_1, \alpha_2, A_y, B_y, C_y, K_{\mu y}) K_{m_1, m_2}(\alpha_1, \alpha_2, A_z, B_z, C_z, K_{\mu z}), \quad (4.9)$$

where

$$K_{n_1, n_2}(\alpha_1, \alpha_2, A_x, B_x, C_x, K_x) = \exp(-H\overline{AB}_x^2) \exp(iK_x \overline{CD}_x) \times \sum_{r_1} \binom{n_1}{r_1} \overline{AD}_x^{n_1 - r_1} \sum_{r_2} \binom{n_2}{r_2} \overline{BD}_x^{n_2 - r_2} F_{r_1 + r_2}(\beta, K_x), \quad (4.10)$$

where

$$F_n(\beta, \kappa) = (2i)^{-n} \pi^{1/2} \beta^{-(n+1)/2} \exp(-\kappa^2/4\beta) H_n(-\kappa/2\sqrt{\beta}) \quad (4.11)$$

and where the  $H_n(\lambda)$  are the Hermite polynomials.

The sum over  $\mathbf{K}_\mu$  can be visualized as a sum over a sphere of radius  $K$  in reciprocal space. Again, use can be made of the factorization displayed in Eq. (4.9): the number of unique reciprocal lattice vectors inside a sphere of radius  $K$  is proportional to  $K^3$  while the number of unique values of  $K_{\mu x}$ ,  $K_{\mu y}$ ,  $K_{\mu z}$  is usually proportional to  $K$ .

### C. The Matrix Elements of $V^c$

The matrix elements of  $V^c$  can be expressed as a lattice sum of three-center integrals of the form

$$V_{n_1 l_1 m_1, n_2 l_2 m_2}^c(\alpha_1, \alpha_2, \delta, \mathbf{A}, \mathbf{B}, \mathbf{C}) = \int \chi_{n_1 l_1 m_1}(\alpha_1, \mathbf{r}_A) (\exp(-\delta r_C^2)/r_C) \chi_{n_2 l_2 m_2}(\alpha_2, \mathbf{r}_B) d\tau. \quad (4.12)$$



These integrals can be easily evaluated to yield

$$\begin{aligned}
 & V_{n_1 l_1 m_1, n_2 l_2 m_2}^c(\alpha_1, \alpha_2, \delta, \mathbf{A}, \mathbf{B}, \mathbf{C}) \\
 &= \pi^{-1/2} e^{-H\overline{AB}^2} \sum_{r_1} \binom{n_1}{r_1} \overline{AB}_x^{n_1-r_1} \sum_{s_1} \binom{l_1}{s_1} \overline{AB}_y^{l_1-s_1} \sum_{t_1} \binom{m_1}{t_1} \overline{AB}_z^{m_1-t_1} \\
 &\quad \times \sum_{r'} \binom{n_2+r_1}{r'} N_{r'} \sum_{s'} \binom{l_2+s_1}{s'} N_{s'} \sum_{t'} \binom{m_2+t_1}{t'} N_{t'} \sum_{r''} \binom{n_2+r_1-r'}{r''} \\
 &\quad \times \overline{BC}_x^{n_2+r_1-r'-r''} \overline{CD}_x^{r''} \beta^{r''} \sum_{s''} \binom{l_2+s_1-s'}{s''} \overline{BC}_y^{l_2+s_1-s'-s''} \overline{CD}_y^{s''} \beta^{s''} \\
 &\quad \times \sum_{t''} \binom{m_2+t_1-t'}{t''} \overline{BC}_z^{m_2+t_1-t'-t''} \overline{CD}_z^{t''} \beta^{t''} \kappa_{(r'+s'+t'+2r''+2s''+2t'')/2}(\beta, \delta, \gamma, \overline{CD}),
 \end{aligned} \tag{4.13}$$

where

$$\begin{aligned}
 \kappa_n(\beta, \delta, \gamma, z) &= \gamma^{-(n+1)} \exp(-\beta\delta z^2/\gamma) \sum_q \binom{n}{q} \\
 &\quad \times (-1)^q \Gamma(q + \frac{1}{2}) \gamma^*(q + \frac{1}{2}, \beta^2 z^2/\gamma), \\
 \gamma &= \alpha_1 + \alpha_2 + \delta,
 \end{aligned} \tag{4.14}$$

and the function  $\gamma^*(a, x)$  is the entire incomplete gamma function [10].

This is the only matrix element that does not factorize. As a result, even though there is just one exponential of this type for each atom in the unit cell, a major portion of the computational effort must be expended in evaluating the matrix elements of  $V^c$ .

Since the only purpose of  $V^c$  is to reproduce the Coulombic singularity, the exponent  $\delta$  in Eq. (4.12) can be chosen to be extremely large. If  $\delta$  is large as discussed above, good results can be achieved by simply fitting the individual terms of  $V^c$  to a sum of Gaussians as first suggested by R. N. Euwena [11]. This yields an expansion of the form

$$e^{-\delta r^2}/r \simeq \sum_n a_n e^{-\lambda_n r^2} \tag{4.15}$$

and the required integrals can then be treated as factorizable and are evaluated in a manner identical to that described in Section IV.A. In the example calculation of a 33-atom copper thin film to be discussed later, a 4-Gaussian fit results in a computational error of 0.7 eV for the copper 1s core state. However, for the conduction bands (which are the states of interest) the error introduced by the approximation is less than 0.002 eV.

## V. RECTANGULAR SYMMETRY

Many crystals have rectangular or cubic symmetry. In addition, many other crystals can be forced to assume such symmetry by simply choosing a larger unit cell. For example, in the case of hexagonal symmetry where the primitive lattice vectors are given by

$$\begin{aligned} \mathbf{a}_1 &= a(\sqrt{3}, -1, 0)/2, \\ \mathbf{a}_2 &= a(0, 1, 0), \\ \mathbf{a}_3 &= c(0, 0, 1), \end{aligned} \quad (5.1)$$

one can force rectangular symmetry by choosing "primitive" lattice vectors

$$\begin{aligned} \mathbf{A}_1 &= 2\mathbf{a}_1 + \mathbf{a}_2 = \sqrt{3}a\hat{x}, \\ \mathbf{A}_2 &= \mathbf{a}_2 = a\hat{y}, \\ \mathbf{A}_3 &= \mathbf{a}_3 = c\hat{z}. \end{aligned} \quad (5.2)$$

The resultant unit cell is twice as large as it needs to be, but rectangular symmetry has been achieved. More importantly, in supercell calculations of surfaces, amorphous materials, or defects, it is almost always possible to choose the supercell to have rectangular symmetry. The presence of rectangular symmetry greatly simplifies the tight-binding calculations.

When rectangular symmetry exists, the lattice vectors can be written as

$$\mathbf{R}_v = v_1 a_1 \hat{x} + v_2 a_2 \hat{y} + v_3 a_3 \hat{z}. \quad (5.3)$$

In such a case, the potential energy term given in Eq. (4.4) becomes

$$\begin{aligned} & \mathbf{X}_{n_1 l_1 m_1, n_2 l_2 m_2}^{n_3 l_3 m_3}(\alpha_1, \alpha_2, \gamma, \mathbf{A}, \mathbf{B}, \mathbf{C}) \\ &= W_{n_1 n_2}^{n_3}(\alpha_1, \alpha_2, \gamma, A_x, B_x, C_x) \\ & \quad \times W_{l_1 l_2}^{l_3}(\alpha_1, \alpha_2, \gamma, A_y, B_y, C_y) W_{m_1 m_2}^{m_3}(\alpha_1, \alpha_2, \gamma, A_z, B_z, C_z) \end{aligned} \quad (5.4)$$

where

$$W_{n_1 n_2}^{n_3}(\alpha_1, \alpha_2, \gamma, A_x, B_x, C_x) = \sum_{v_1} U_{n_1 n_2}^{n_3}(\alpha_1, \alpha_2, \gamma, A_x, B_x, C_x - v_1 a_1). \quad (5.5)$$

In this way, a lattice sum over  $N^3$  terms can be reduced to three summations of only  $N$  terms each. All other factorizable integrals of overlap, kinetic energy, and potential energy can be treated in an identical manner.

The simplification introduced by rectangular symmetry goes further than this.

The multicenter integrals do not need to be evaluated at all. What is actually desired is the matrix elements of the secular equation of Eq. (2.16). For the case of rectangular symmetry, the matrix element for the above example, evaluated at point  $\mathbf{k}$  in the Brillouin zone, can be written in factorized form as

$$\begin{aligned} & \sum_{\mathbf{v}} e^{i\mathbf{k} \cdot \mathbf{R}_{\mathbf{v}}} \mathbf{X}_{n_1 l_1 m_1, n_2 l_2 m_2}^{n_3 l_3 m_3}(\alpha_1, \alpha_2, \gamma, \mathbf{A}, \mathbf{B} - \mathbf{R}_{\mathbf{v}}, \mathbf{C}) \\ &= \left[ \sum_{v_1} \exp(ik_x v_1 a_1) W_{n_1 n_2}^{n_3}(\alpha_1, \alpha_2, \gamma, A_x, B_x - v_1 a_1, C_x) \right] \\ & \quad \times \left[ \sum_{v_2} \exp(ik_y v_2 a_2) W_{l_1 l_2}^{l_3}(\alpha_1, \alpha_2, \gamma, A_y, B_y - v_2 a_2, C_y) \right] \\ & \quad \times \left[ \sum_{v_3} \exp(ik_z v_3 a_3) W_{m_1 m_2}^{m_3}(\alpha_1, \alpha_2, \gamma, A_z, B_z - v_3 a_3, C_z) \right]. \quad (5.6) \end{aligned}$$

Thus the individual multicenter integrals do not need to be evaluated and only the  $W$ -matrices need to be calculated and permanently stored. Not only does this increase the speed of computation, but just as importantly, this procedure vastly reduces the amount of information which must be stored.

Although only the matrix elements of  $V^g$  were analyzed in the above example, it is clear that the same factorization occurs for the matrix elements of overlap, kinetic energy, and  $V^k$ . If the expansion technique of Eq. (4.15) is employed, then the matrix elements of  $V^c$  can also be factorized. Additionally, it should also be noted that this formalism is ideal for vector processing.

## VI. APPLICATION TO COPPER THIN FILM

As an example of the power and speed of this technique, a calculation of the electronic band structure of a 33-atom thick (100) copper thin film using the Chodorow [12] potential is presented here. The original tabular potential of Chodorow was least-squares fit to the functional form of Eq. (2.11) with  $n = l = m = 0$ . This potential was chosen in order to permit the results of this calculation to be directly compared with Burdick's [12] calculation of bulk copper (one atom/cell) and with a Slater-Koster interpolation for a copper thin film (33 atoms/cell) performed by Sohn *et al.* [13]. Following the notation of Eqs. (2.7)–(2.12), the potential used is characterized by

$$\begin{aligned} \delta_1 &= 10^5, \\ U_{\mu}^k &= \begin{cases} -0.47425 & \text{for } \mathbf{K}_{\mu} = 0 \\ 0 & \text{otherwise} \end{cases}, \end{aligned}$$

TABLE I  
Coefficients of Gaussian Portion of Chodorow Potential

$i$	$(\sigma_1^{000})_i$	$\gamma_i$
1	166.266	1.03786
2	-545.970	1.18583
3	938.788	1.50391
4	-1289.78	2.03274
5	1564.23	2.83552
6	-1803.68	4.01895
7	1972.56	5.71692
8	-2242.34	8.18403
9	2319.53	11.4168
10	-2613.09	16.5669
11	1982.40	21.3932
12	-2167.83	37.9455
13	1856.66	44.7698
14	-2405.29	68.5732
15	1948.51	67.3400
16	-353.397	316.602
17	-724.562	1133.56
18	-1630.57	4519.20
19	-4229.24	21993.8

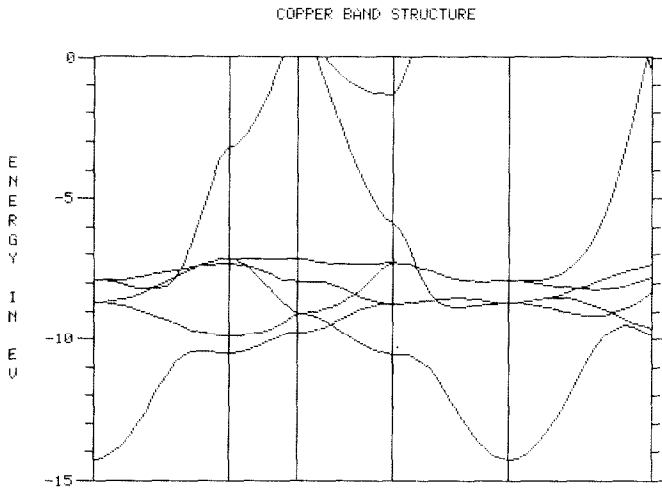


FIG. 1. Band structure of bulk copper (1 atom/cell).

TABLE II  
Gaussian Fit to Singular Portion of Chodorow  
Potential

$n$	$a_n$	$\lambda_n$
1	-116198.0	9774530.0
2	-33478.90	1463280.0
3	-14743.30	339249.00
4	-9409.770	119107.00

and where the  $19 \sigma_1^{000}$  coefficients and their associated  $\gamma$ 's are given in Table I. For this potential, the band structure of bulk copper (one atom per unit cell) was computed and compared with Burdick. The largest disagreement was 0.16 eV and the rms error was 0.05 eV. These small discrepancies are probably due to the failure of the fitted potential to exactly reproduce a muffin-tin function. This bulk band structure is shown in Fig. 1.

Of more interest is the calculation of the 33 atoms/cell copper thin film—for the computational burden increases dramatically as one increases the number of atoms in the unit cell. For this thin film calculation, the  $U^c$  term, in accordance with Eq. (4.15), was replaced by a sum of four Gaussians. The coefficients of this fit are given in Table II. The orbital exponents,  $\alpha_i$ , are those reported by Wachters [14]. None of Wachters' exponents were omitted as is frequently done in order to reduce the computational burden. The computed band structure is shown in Fig. 2 and a

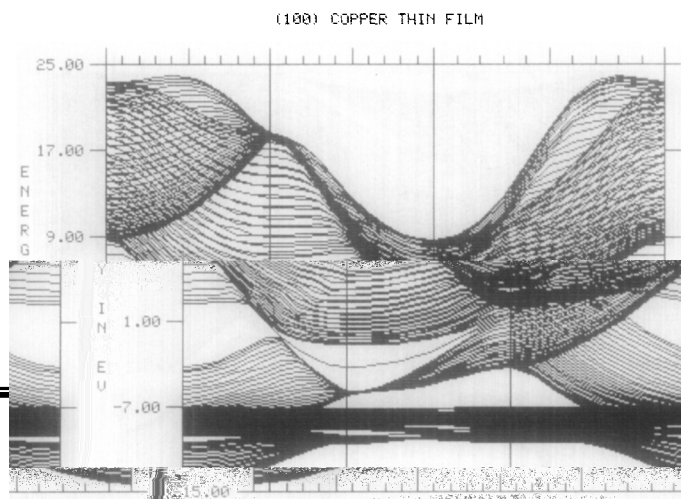


FIG. 2. Band structure of copper 100 thin film (33 atoms/cell).

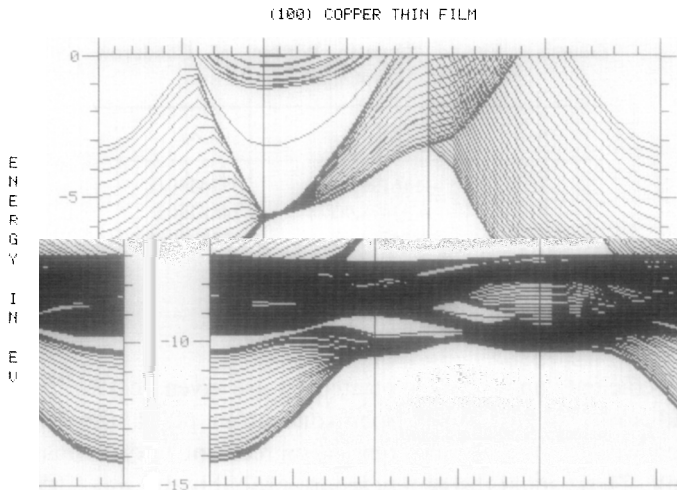


FIG. 3. Band structure of copper 100 thin film—region about Fermi energy.

magnified view of the region about the Fermi energy is shown in Fig. 3. The *d*-band region is shown in Fig. 4. These figures compare quite favorably with the results of Sohn *et al.* [13]. Mulliken population analysis clearly shows the existence of results are not self-consistent and are presented here only to illustrate the capacity of the programs so far developed. The advantage of the technique presented here over that employed by Sohn *et al.* is that, unlike the Slater-Koster interpolation

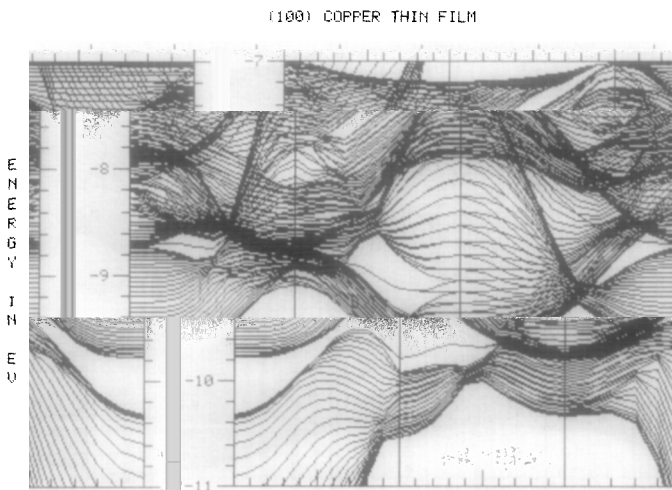


FIG. 4. Band structure of copper 100 thin film—the *d*-band region.

scheme, this first-principles calculation can be carried to self-consistency. Again none of the potential exponents nor the Gaussian orbital exponents were removed in order to reduce the computational burden. The time required to compute all the multicenter integrals (or those quantities which replace the multicenter integrals) of overlap, kinetic energy, and potential energy was approximately 5 CPU h on an IBM 3081K machine (15 mips).

Many of the approximations often used (such as removing the long-range exponents as mentioned above) no longer need to be made and a higher criterion of accuracy can be demanded in the lattice sums. Empirically it is found that this results in a less ill-conditioned secular equation and a significantly higher degree of accuracy in the energies and wavefunctions produced.

## VII. SUMMARY AND CONCLUSIONS

A family of programs has been developed which takes advantage of this factorized tight-binding (FTB) formulation. Full use of rectangular symmetry, when it exists, is employed. These programs are specifically directed to the treatment of surfaces and interfaces and it is in these areas that the formulation introduced here can be applied to maximum advantage. These programs are, however, general in nature and entirely symmetry independent. As a result they can be applied to any crystalline problem. To date, these programs have been successfully applied to copper (one atom/unit cell), silicon (two atoms/unit cell), alpha quartz (nine atoms/unit cell), berlinite (18 atoms/unit cell), a (100) copper surface (33 atoms/unit cell), and a treatment of an oxygen vacancy in quartz (72 atoms/unit cell). Empirically, it is found that the simplifications introduced by this formulation translate, in machine

---

it should be noted that this same factorization scheme can also be applied to the calculation of the electronic charge density over a rectangular mesh within a unit cell.

## ACKNOWLEDGMENT

The author wishes to thank professor John Chandler of the Computer Science Department of Oklahoma State University for his invaluable assistance.

## REFERENCES

1. F. BLOCH, *Z. Physik* **52**, 555 (1928).
2. E. E. LAFON AND C. C. LIN, *Phys. Rev.* **152**, 579 (1966).
3. D. W. BULLETT, *Solid State Phys.* **35**, 129 (1980).
4. W. Y. CHING AND J. CALLAWAY, *Phys. Rev. B* **9**, 5115 (1974).

5. R. HEATON AND E. LAFON, *Phys. Rev. B* **17**, 1958 (1978).
6. MEHTA-AJMANI, I. BATRA, E. E. LAFON, AND C. S. FADLEY, *J. Phys. C* **13**, 2807 (1980).
7. J. K. MACDONALD, *Phys. Rev.* **43**, 830 (1933).
8. R. C. CHANEY, T. K. TUNG, C. C. LIN, AND E. E. LAFON, *J. Chem. Phys.* **52**, 361 (1970).
9. C. S. WANG AND J. CALLAWAY, *Comput. Phys. Commun.* **14**, 327 (1978).
10. J. SPANIER AND K. B. OLDHAM, *An Atlas of Functions* (Hemisphere, New York, 1987), p. 435.
11. R. N. EUWEMA, private communication.
12. G. A. BURDICK, *Phys. Rev.* **129**, 138 (1963).
13. K. S. SOHN, D. G. DEMSEY, L. KLEINMAN, AND E. CAURUTHERS, *Phys. Rev. B* **13**, 1515 (1976).
14. A. J. H. WACTHERS, *J. Chem. Phys.* **52**, 1033 (1970).
15. E. LAFON, MIT Solid State and Molecular Theory Group Quarterly Progress Report No. 69, p. 66, 1968 (unpublished).
16. K. MEDNICK AND C. C. LIN, *Phys. Rev. B* **17**, 4807 (1978).